Technology and electrophysical properties of Mn^{4+}, Sb^{3+}, Dy^{3+} and W^{6+} -doped $Pb(Zr_{0.49}Ti_{0.51})O_3$ ceramics

Dariusz Bochenek[1,a], Ewa Ćwikiel[1], Przemysław Niemiec[1] and Tomasz Goryczka[2]

[1] *University of Silesia in Katowice, Faculty of Computer Science and Material Science, Institute of Technology and Mechatronics 12, Żytnia St., 41–200, Sosnowiec, Poland*
[2] *University of Silesia in Katowice, Faculty of Computer Science and Material Science, Institute of Material Science, 1a, 75 Pułku Piechoty St., 41–500 Chorzów, Poland*

Abstract. In paper three multicomponent PZT-type ceramics doped by Mn^{4+}, Sb^{3+}, Dy^{3+}, W^{6+} have been prepared by the conventional mixed oxide method. The multicomponent PZT-type ceramic powders were synthetized by calcining route, while densification was carried out by pressureless sintering method. The paper presents XRD, SEM, EDS, dielectric and DC electric conductivity measurements of the multicomponent PZT-type ceramic samples. Conducted tests indicate obtained multicomponent PZT-type exhibit good dielectric properties giving the possibility for their use as actuators and piezoelectric transducers in modern micromechatronic and microelectronic applications.

1 Introduction

Ceramic materials prepared on the basis of lead zirconate titanate $Pb(Zr_{1-x}Ti_x)O_3$ (PZT-type ceramics in short) are one of the most studied ferroelectric materials, due to its extremely wide field of electronic 'smart' applications including sensors, actuators, transducers, transformers, electric resonators, speakers, nonvolatile or computer memories, display, MEMS devices etc. [1-5]. The properties of PZT-type ceramics depend on the ratio of Zr^{4+}/Ti^{4+} and on the admixtures introduced to the base composition [6-10, 11]. In the room temperature pure PZT has ferroelectric properties (so it possesses also piezo and pyroelectric properties) for: $0.042<x<0.380$ (rhombohedral phase R*3c*), $0.380<x<0.470$ (rhombohedral phase R*3m*) as well as $0.480<x<1.000$ (tetragonal phase P*4mm*) [5, 12]. PZT solid solutions from the area of $0.47<x<0.48$ is called morphotropic phase boundary region (MPB). PZT ceramic materials with compositions near to the MPB reveal excellent electromechanical properties [13-15].

Dopants are added to PZT material in order to enhance the electrophysical properties. Additives alter the defect structure of the PZT lattice and give the opportunity to tailor the electrophysical properties in a wide range. Is common practice in planning new compositions to use more than one type of dopants to the given composition in order to achieve the appropriate set of properties [16]. Appropriate choice of a type and a quantity of dopant ions is important.

In the research the multicomponent PZT-type ceramics doped by manganese Mn^{4+}, antimony Sb^{3+}, dysprosium Dy^{3+} and tungsten W^{6+} were obtained and investigated.

[a] dariusz.bochenek@us.edu.pl

The three chemical compositions:
$Pb(Zr_{0.49}Ti_{0.51})_{0.94}Mn_{0.021}Sb_{0.016}Dy_{0.012}W_{0.012}O_3$ (PZT-1),
$Pb(Zr_{0.49}Ti_{0.51})_{0.94}Mn_{0.021}Sb_{0.016}Dy_{0.010}W_{0.013}O_3$ (PZT-2),
$Pb(Zr_{0.49}Ti_{0.51})_{0.94}Mn_{0.021}Sb_{0.016}Dy_{0.008}W_{0.014}O_3$ (PZT-3),
were designed and obtained, at following technological conditions: T_s= 1170°C/t_s=2 h.

The aim of this study was obtained and examined Mn^{4+}, Sb^{3+}, Dy^{3+} and W^{6+} - doped $Pb(Zr_{0.49}Ti_{0.51})O_3$ multicomponent ceramic materials for modern microelectronic and micromechatronic applications.

2 Experimental details

2.1 Technology and sample preparation

Ceramic samples of the multicomponent PZT-type materials were prepared by the conventional mixed oxide method. The starting powders PbO (99.99 %, POCH), ZrO_2 (99.00 %, Merck), TiO_2 (99.99 %, Merck), MnO_2 (90 %, Merck), Sb_2O_3 (99.995 %, Aldrich), Dy_2O_3 (99.9%, Aldrich), and WO_3 (99.9 %, Fluka) were milled for 24 h in ethanol using ZrO_2 balls. After drying the mixtures of powders were calcined in air at following conditions T_{calc}= 850°C for t_{calc}= 4 h, at heating rate of 150°C/h. An additional 5.0 wt.% PbO was added to compensate for its evaporation during calcination and densification. Densification (sintering) was carried out by the conventional method (pressureless sintering method). Disks 10 mm in diameter and 1 mm in thickness were pressed and next were sintered in closed alumina crucibles at following sintering conditions: T_s= 1170°C / t_s=2 h (a heating rate of 150°C/h). The final steps of

technology were grinding, polishing, removing mechanical stresses (annealing was performed at temperature at following conditions: 700°C/15 min.) and for electrical testing the surfaces of the samples were covered with a silver electrode.

2.2 Characterization

X-ray measurements were carried out at room temperature using X'Pert-Pro PW3040/60 diffractometer. The copper radiations $CuK_{\alpha 1}/_{\alpha 2}$ were used. The X-ray diffraction patterns were stored at range of 2θ from 10° to 130° in step-scan mode: 0.05 degrees and 4 s/step.

The chemical composition and microscope observation of the samples were done using JEOL JSM-7100 TTL LV Field Emission Scanning Electron Microscope equipped with Energy Dispersive Spectrometer (EDS).

Temperature studies of the dielectric properties were made using a QuadTech 1920 Precision LCR Meter at temperature range from 20°C to 450°C (heating cycle, heating rate of 1.0 deg./min., frequency range of the measurement field from 20 Hz to 1 MHz). Measurements of DC electric conductivity were made using a 6517B Keithley electrometer in the temperature range from 20°C to 450°C (for 5 V).

3 Results and discussion

3.1. X-ray diffraction analysis

Fig. 1 shows comparison of the X-ray diffraction patterns measured for the multicomponent PZT-type ceramics at room temperature (T_r). The first of all, X-diffraction lines, presented in the patterns, were identified as a one belonging to the perovskite type of structure with tetragonal crystal lattice.

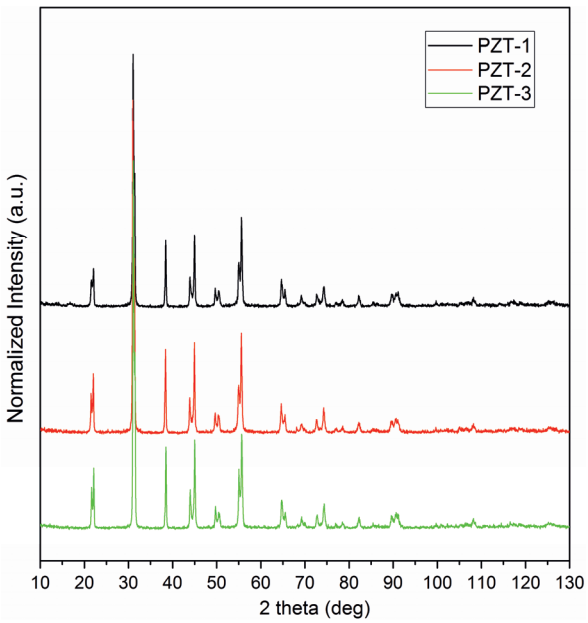

Figure 1. X-ray diffraction patterns of the multicomponent PZT-type ceramics.

All the PZT-type materials were a single phase without the presence of substrate phases or other equilibrium one. In order to determine the lattice parameters, the X-ray diffraction patterns were fitted using the Rietveld method [17]. Data for the starting model were received from ICDD data base for polymorphic phase: $Ba_{0.8}Pb_{0.2}TiO_3$ (card no. 074-2492). Symmetry of the crystal lattice can be described using space group *P4mm*. Results of determined lattice parameters were shown in Table 1.

Table 1. Values of the parameters of the multicomponent PZT-type samples (dielectric studies were carried out for ν=1 kHz).

	PZT-1	**PZT-2**	**PZT-3**
ρ (g/cm^3)	6.96	6.81	7.05
a_0 (Å)	4.0343	4.0363	4.0371
b_0 (Å)	4.0343	4.0363	4.0371
c_0 (Å)	4.1225	4.1249	4.1258
V_0 (Å^3)	67.09	67.20	67.24
T_C (°C)	284	290	296
ε_r at T_r	447	848	680
ε_{max} at T_C	8486	15990	12386
tanδ at T_r	0.003	0.002	0.004
tanδ at T_C	0.122	0.089	0.104
ρ_{DC} at T_r (Ωm)	3.4 x10^9	4.7 x10^8	5.3 x10^7

3.2. Microstructural and EDS tests

Fig. 2 shows the microstructural SEM images of the PZT-type compositions which prove that the technological process has been properly carried out and correctly selected technological conditions.

On the SEM microstructural image, the PZT-1 ceramic sample (with the largest amount of dysprosium and the smallest amount of tungsten) ceramic grains exhibit a correct angular shape witch large size (Fig. 2a). The grain boundaries of the PZT-1 ceramics have regular shapes. The fracture of the PZT-1 ceramic sample occurs mainly along the grain boundary, and in a small percentage the fracture is also carried out through the grain.

In the case of the PZT-2 ceramic sample (with the intermediate amount of tungsten and dysprosium dopant) an increase in the heterogeneity of the microstructure grains is observed (Fig. 2b). The microstructure of the PZT-2 ceramics also has grains with non-sharp edges and irregular shape of grain boundaries and the fracture occurs both on the grain boundaries and through the grains. In case of the PZT-3 ceramics the microstructure appearance is similar to the microstructure of the PZT-1 ceramics.

The PZT-type ceramic samples were subjected to composition homogeneity tests by spectroscopy with EDS energy dispersion (Fig. 3) based on point and surface analysis. The EDS tests confirmed the qualitative composition of the obtained samples without the presence of foreign elements. Summarized in the Table 2 theoretical (Theor.) and calculated (Exptl.) the percentage

of the individual components of the PZT-type ceramics (the average of ten randomly chosen areas from the specimen surface). In the case all samples, zirconium, titanium and introduced admixtures (i.e. manganese, antimony and tungsten) deficiency are observed compared to theoretical calculations. In the same time an excess of lead and dysprosium are observed. All deviations from the initial composition are within the acceptable range.

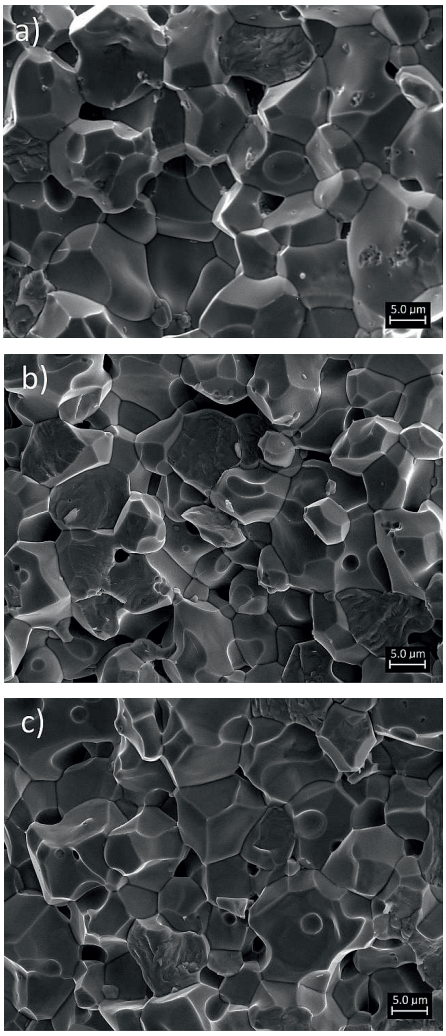

Figure 2. SEM images of the microstructure of PZT-type sample fractures: a) PZT-1, b) PZT-2, c) PZT-3.

Table 2. Theoretical and experimental percentages of elements of PZT-type ceramics.

	PZT-1		PZT-2		PZT-3	
	Theor. (%)	Exptl. (%)	Theor. (%)	Exptl. (%)	Theor. (%)	Exptl. (%)
PbO	66.60	71.66	66.63	70.92	66.67	71.88
ZrO_2	18.02	14.52	18.03	14.39	18.03	14.51
TiO_2	12.16	10.53	12.17	11.69	12.17	11.08
MnO_2	0.58	0.44	0.58	0.47	0.58	0.49
Sb_2O_3	0.78	0.70	0.85	0.64	0.93	0.60
Dy_2O_3	0.83	1.4	0.71	1.25	0.59	0.76
WO_3	1.03	0.74	1.03	0.64	1.03	0.69

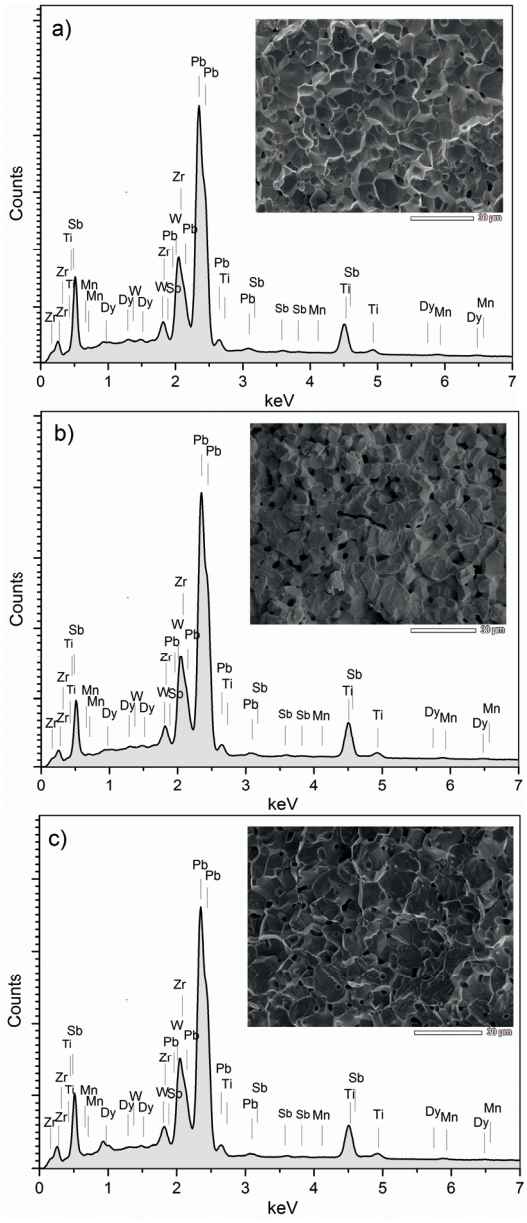

Figure 3. The EDS analysis image of the element distribution for the multicomponent PZT-type ceramics: a) PZT-1, b) PZT-2, c) PZT-3.

3.3 Dielectric properties and DC conductivity

Temperature measurements of the dielectric permittivity of the multicomponent PZT-type materials at frequency 1 kHz are presented in Fig. 4a. All obtained compositions show high values of dielectric permittivity with a clear, sharp phase transition (from the ferroelectric phase to the paraelectric one). At room temperature, the values of the dielectric permittivity are in the range of 447 to 848 (Table 1).

The highest values of the dielectric permittivity maximum show the PZT-2 ceramic sample (with intermediate amounts of tungsten and dysprosium admixtures in its chemical composition). From the group of obtained compositions the lowest values of the dielectric permittivity maximum are shown by the

composition of PZT-1 (with the largest amount of dysprosium and the smallest amount of tungsten).

The multicomponent PZT-type ceramics are characterized by low dielectric loss (Fig. 4b). In the area of phase transition, there is a local maximum of the dielectric loss. It is characteristic for multicomponent PZT materials with a perovskite-like structure. Above temperature of 350°C there is a rapidly increase in dielectric loss associated with an increase in electrical conductivity at higher temperatures.

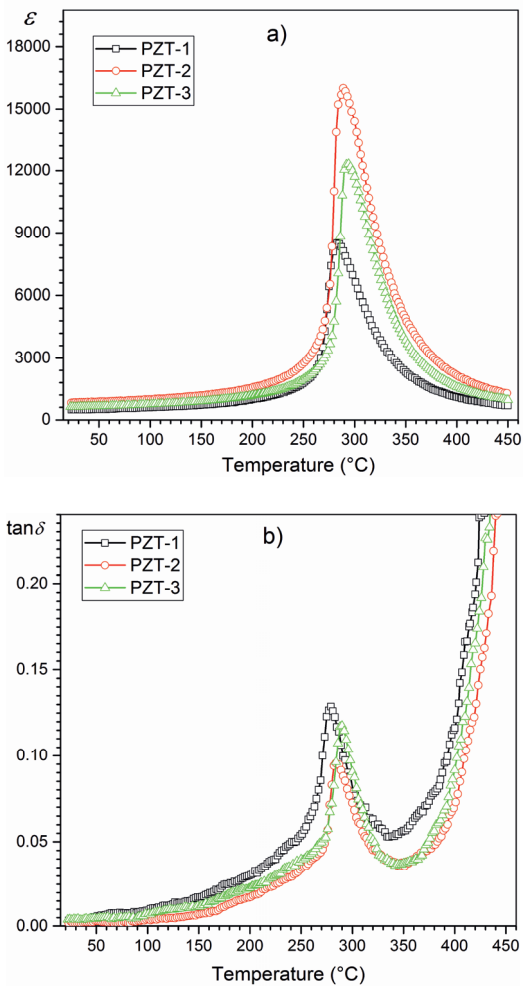

Figure 4. Temperature dependencies of the $\varepsilon(T)$ (a) and $\tan\delta(T)$ (b) for multicomponent PZT-type ceramics (a heating cycle), at frequency 1 kHz.

The frequency dependencies (in the frequency range from 20 Hz to 1 MHz) of dielectric permittivity at various temperatures (from 25°C to 400°C) of the multicomponent PZT-type ceramics are shown in Fig. 5. The values of dielectric permittivity decreases with the increase of frequency (in frequency region from 20 Hz to 5 kHz), and it attains a constant value at high frequencies. This phenomenon is typical for a Maxwell-Wagner type of interfacial polarization.

Fig. 6 shows the temperature dependencies of $\ln\sigma_{DC}(1000/T)$ for the multicomponent PZT-type materials. The DC electrical conductivity tests showed that all PZT-type ceramics have similar waveforms. As the temperature increases, the direct current conductivity increases, too. The research showed no clear trend related to the variable amount of tungsten and dysprosium in the basic PZT-type composition.

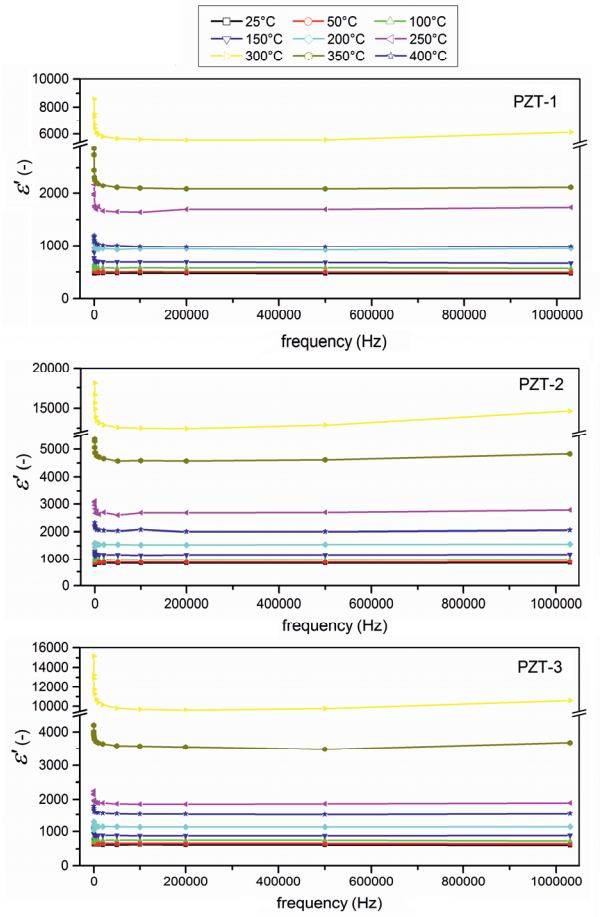

Figure 5. Frequency dependencies of dielectric permittivity of the multicomponent PZT-type ceramics.

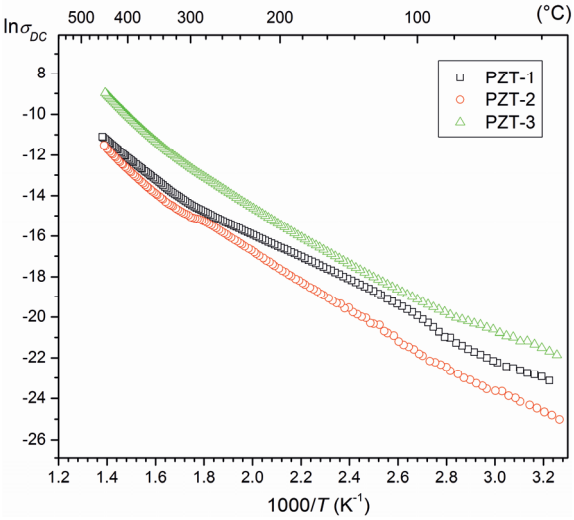

Figure 6. The $\ln\sigma_{DC}(1000/T)$ dependencies multicomponent PZT-type ceramics.

4 Conclusion

In paper three multicomponent PZT-type ceramics doped by Mn^{4+}, Sb^{3+}, Dy^{3+}, W^{6+} have been designed and obtained at following technological conditions: T_s= 1170°C/t_s=2 h.

Results obtained from the X-ray diffraction confirmed single-phase state of the PZT with the perovskite type structure and tetragonal crystallographic system. The microstructures of the multicomponent PZT-type compositions prove that the technological process has been properly carried out and correctly selected technological conditions (ceramic grains exhibit a correct angular shape). All obtained compositions show high values of dielectric permittivity with a sharp ferroelectic-paraelectric phase transition as well as very low dielectric loss.

The good electrophysical properties of the multicomponent PZT-type ceramics, allowed using this type materials as an element to build actuators and piezoelectric transducers in modern micromechatronic and microelectronic devices.

References

1. Z.-G. Ye, *Handbook of Advanced Dielectric, Piezoelectric and Ferroelectric Materials. Synthesis, Properties and Applications* (Woodhead Publishing and Maney Publishing, Cambridge 2008)
2. P.-H. Xiang, X.-L. Dong, H. Chen, Z. Zhang, J.-K. Guo, Ceram. Int. **29**, 499 (2003)
3. V.R. Mudinepalii, R.K. Sirugudu, N. Ramamanohar Reddy, K.V. Sivakumar, V.R.K. Murthy, B.S. Murty, Mater. Chem. Phys. **126**, 295 (2011)
4. J. Li, Q. Sun, Rare Metals **27**, 362 (2008)
5. B. Jaffe, R. Cook, H. Jaffe, *Piezoelectric Ceramics*, (Academic Press, New York, 1971)
6. H. Wei, Y. Chen, Ceram. Int. **41**, 6158 (2015)
7. W. Qiu, H. H. Hng, Mater. Chem. Phys. **75**, 151 (2002)
8. D. Bochenek, P. Niemiec, M. Adamczyk, R. Skulski, R. Zachariasz, B. Wodecka-Duś, Z. Machnik, Arch. Metall. Mater. **62**, 667 (2017)
9. E. Boucher, B. Guiffard, L. Lebrun, D. Guyomar, Ceram. Int. **32**, 479 (2006)
10. L. Kozielski, M. Adamczyk, N. Schreithofer, W. Sakamoto, R. Nowak, Jpn. J. Appl. Phys. **47**, 2176 (2008)
11. R. Zachariasz, D. Bochenek, K. Dziadosz, J. Dudek, J. Ilczuk, Arch. Metall. Mater. **56**, 1217 (2011)
12. D. Bochenek, P. Niemiec, R. Zachariasz, A. Chrobak, G. Ziółkowski, Arch. Metall. Mater. **58**, 1013 (2013)
13. A. Bouzid, E.M. Bourim, M. Gabbay, G. Fantozzi, J. Eur. Ceram. Soc. **25**, 3213 (2005)
14. N. Izyumskaya, Y. I. Alivov, S. J. Cho, H. Morkoç, H. Lee, Y. S. Kang, Crit. Rev. Solid State **32**, 111 (2007)
15. A.J. Moulson, J.M. Herbert, *Electroceramics: Materials, Properties, Applications* (second ed., Wiley, Chichester, West Sussex, 2003)
16. N. Texier, Ch. Courtois, M. Traianidis, A. Leriche, J. Eur. Ceram. Soc. **21**, 1499 (2001)
17. M. Morawiec, A. Grajcar, Journal of Achievements in Materials and Manufacturing Engineering **80**, 11 (2017)